Stabilization of Rocky Flats Pu-contaminated ash within chemically bonded phosphate ceramics*

A. S. Wagh, ** **R. Strain, S. Y. Jeong, D. Reed,† T. Krause,† and D. Singh**
Energy Technology Division, †Chemical Technology Division
Argonne National Laboratory
9700 S. Cass Avenue
Argonne, IL 60439, USA

Revised
September 1998

Paper prepared for submission to Journal of Nuclear Materials.

*Project supported by U.S. Department of Energy, Office of Technology Development, as part of the Mixed Waste and Plutonium Focus Areas effort, under Contract W-31-109-Eng-38.

**Corresponding author Tel.: 630-252-4295; fax: 630-252-3604;
e-mail: arun_wagh@qmgate.anl.gov.

Stabilization of Rocky Flats Pu-contaminated ash within chemically bonded phosphate ceramics

A. S. Wagh, R. Strain, S. Y. Jeong, D. Reed,† T. Krause,† and D. Singh
Energy Technology Division, †Chemical Technology Division
Argonne National Laboratory
9700 S. Cass Avenue
Argonne, IL 60439, USA

Abstract

A feasibility study was conducted on the use of chemically bonded phosphate ceramics for stabilization of combustion residue of high transuranic (TRU) wastes. Using a matrix of magnesium potassium phosphate formed by the room-temperature reaction of MgO and KH_2PO_4 solution, we made waste forms that contained 5 wt.% Pu to satisfy the requirements of the Waste Isolation Pilot Plant. The waste forms were ceramics whose compression strength was twice that of conventional cement grout and whose connected porosity was ≈50% that of cement grout. Both surrogate and actual waste forms displayed high leaching resistance for both hazardous metals and Pu. Hydrogen generation resulting from the radiolytic decomposition of water and organic compounds present in the waste form did not appear to be a significant issue. Pu was present as PuO_2 that was physically microencapsulated in the matrix. In the process, pyrophoricity was removed and leaching resistance was enhanced. The high leaching resistance was due to the very low solubility of PuO_2 coupled with superior microencapsulation. As a result, the waste forms satisfied the current Safeguard Termination Limit requirement for storage of TRU combustion residues.

1. Introduction

Several U.S. Department of Energy (DOE) sites store transuranic (TRU) wastes that contain incinerated residues such as ash and ash heels, i.e., ash calcined to eliminate the loss-on-ignition fraction for safe transportation, and Pu-contaminated crucibles [1]. Some of these wastes contain as much as 17 wt.% Pu and require stabilization for their safe transportation, safeguarding, and storage at facilities such as the Waste Isolation Pilot Plant (WIPP). Earlier attempts to stabilize such waste streams [2,3] employed thermal treatments that were based on encapsulating wastes in a dense and hard ceramic or glass matrix. Such heat treatment of TRU wastes is generally expensive. Formation of a good monolithic glass may also be difficult because hot spots develop in the matrix due to pyrophoric components of the waste streams. In addition, if the TRU wastes also contain hazardous components, then release of off-gases containing volatile species of the hazardous metals during heat treatment is always a concern. For these reasons, the search for room-temperature or slightly elevated temperature stabilization methods such as cement grouts and FUETAP (fabricated under elevated temperature and pressure) cements [4] has been actively pursued.

In recent years, we have developed a novel room-temperature stabilization process called chemically bonded phosphate ceramics (CBPCs) for stabilization of low-level mixed wastes [5,6]. Its applications have been extended to stabilization of fission products [7] and macroencapsulation of irradiated lead bricks and debris waste [8]. Current studies indicate that CBPCs may be used to stabilize wastes containing high concentrations of salts that are difficult to stabilize by other methods [9]. Here, we have extended this study to explore their applications for treatment of TRU wastes.

Despite the earlier success of the CBPC process in treating a wide variety of wastes, its suitability for treating TRU wastes containing high levels of Pu is not obvious. Several basic issues need to be addressed. At high Pu loadings, it is necessary to demonstrate that a suitable monolithic waste form can indeed be formed at room temperature by chemical reaction. Because leachability of the radioactive contaminants may be a function of the waste loading and concentration of the

contaminants in the final waste form, the same leaching resistance found for the low-level mixed wastes may not be available at high loadings of Pu.

In addition, several other issues in Pu storage become important in such a study; one of the more important issues is that of gas generation. The presence of radionuclides in cementious or concrete waste forms, which are analogous to CBPCs, may result in the production of gases (primarily H_2 and, to a lesser extent, O_2). Details of such gas generation studies in other waste forms have been reported by McDaniel and Delzer [4], Bibler and Orebaugh [10], Dole et al. [11], Dole and Friedman [12], and Siskind [13]. If organic wastes (e.g., cellulose, rubber, polyvinyl chloride, polyethylene, etc.) are present, other gases such as CO, CO_2, CH_4, and other hydrocarbons, in addition to H_2, may also be generated by radiolytic processes. Details of such studies may be found in articles by Kazanjian [14], Molecke [15], Reed et al. [16], and Reed and Molecke [17] and Reed et al. [18].

Alpha decay due to Pu is primarily responsible for radiolytic gas generation. Accumulation of these gases within the dead volume of the waste canister containing the processed nuclear waste could pose a hazard during the near term, i.e., during processing, transportation, and both interim and long-term storage of nuclear waste. In the near term, the primary concern is that the accumulation of gases, e.g., H_2 and volatile organic compounds, in the dead volume of the waste canister could produce a flammable gas mixture (4% H_2 by volume in air [19, 20]). The long-term concern is that this gas may lead to (a) a potential failure of the canister [4], or (b) contribute to overall gas generation within the repository [21], although a performance assessment by Brush [22] concluded that radiolytic gas generation is not a significant issue for the WIPP. In addition, the high TRU presence may affect the setting reaction and exothermic heat generation during formation of the ceramic waste forms. We have performed a bench-scale study to investigate these issues.

The investigations were done in two phases. To investigate the feasibility of applying the process to high-Pu wastes and to modify the process suitably, we used a surrogate Ce-containing waste formulation that closely resembled the actual Pu waste. The bench-scale surrogate waste

forms were subjected to physical and leaching tests and their performance was evaluated. This allowed us to optimize the binder composition. A typical 2-L (WIPP-size) sample was then made to ensure that scale-up did not pose problems due to excess heat generation as a result of the exothermic reaction that forms these ceramics. The resulting process was then used for the treatability study of two different waste streams: a Pu-U alloy obtained from Argonne's inventory stored in powder form and Rocky Flats ash remaining from an earlier study. The waste forms were made at bench scale and subjected to various physical and leaching tests to assess their performance and detailed gas release studies were conducted.

2. Experimental procedure

Formation of CBPC waste forms is based on an exothermic acid-base reaction between magnesium oxide (MgO) and monopotassium phosphate (KH_2PO_4). The reaction is governed by

$$MgO + KH_2PO_4 + 5H_2O \text{ ----> } MgKPO_4 \cdot 6H_2O. \quad (1)$$

This reaction yields a hard and dense ceramic of magnesium potassium phosphate hydrate (MKP) that acts as a crystalline host matrix for the waste. Details of this process, general characteristics of the matrix, and its applications in low-level and fission product stabilization may be found in Refs. [5 -8]. During the reaction given in Eq. 1, the hazardous and radioactive contaminants also react with KH_2PO_4 to form highly insoluble phosphates. The bulk ceramic will then encapsulate the reacted contaminants in the dense crystalline matrix of MKP.

Because the bound water in the reaction product may affect the total radiolytic hydrogen generation, its content in the matrix was evaluated by differential thermal and thermogravimetric analyses. The results are given in Fig. 1.

Our initial investigation involved study with the surrogate waste stream given in Table 1 that simulated the actual waste stream very closely. Because Ce is chemically similar to Pu and U (i.e., similar oxidation states and nearly the same ionic radii for those states), we used CeO_2 as a

surrogate of PuO_2 in actual waste. Behrens et al. [1] showed that the actual TRU combustion residues contain Pu as PuO_2, with only a small fraction of a reduced phase. Neodymium (Nd) was used as the surrogate of a small accumulation of americium (Am) that is formed by disintegration of Pu. Combustion residues are typically mixed wastes, i.e., they also contain hazardous metals (defined by the Resource Conservation and Recovery Act [23]) such as Ba, Cr, Ni, Cu, and Pb. They must be stabilized to pass the Toxicity Characteristics Leaching Procedure (TCLP) [24] as a part of the land disposal restrictions [25]. For these reasons, oxides of these metals were added in the surrogate waste. Other components in the wastes are common metal compounds, represented by the respective oxides, and carbon. Because the combustion residues contain a significant amount of carbon, this simulated waste is added with activated carbon, which also represents the carbon often used as an adsorbent for the contaminated liquid fraction of the waste.

Analytical-grade MgO used in this study was supplied by Mallinckrodt as the dead burnt oxide. It was further calcined to reduce its reactivity. Food-grade KH_2PO_4 was obtained from FMC Corporation. Both were combined in a vibratory mixer for several hours. The surrogate waste and the mixture of the binder powder were mixed with water in a Hobart tabletop mixer; the powders were added to the water. The ratio of surrogate waste to the entire content of the mixture was such that the Ce content would be 5 wt.%, which is the safeguard limit for Pu in the final waste form as described in the Pu Recoverability Testing procedure of DOE [26]. The entire process was carried out in a nitrogen glovebox at atmopheric pressure so that the processing conditions simulated the actual environment needed for Pu stabilization. Because the nitrogen fed in the glovebox was dry gas, some evaporation of the water during mixing was inevitable. To compensate for this water loss, we added an additional 30 wt.% water in the mixture over that required by the stoichiometric amount determined by Eq. 1.

The content was mixed for ≈30 min at the lowest mixer speed. Initially, the slurry cooled slightly as the phosphate content of mixture began to dissolve in the water. Subsequently, as the reaction between MgO and dissolved KH_2PO_4 started, the slurry began to warm back to room

temperature, reaching that point after 30 min of mixing. Mixing was then stopped and the slurry was transferred into polyethylene cylindrical molds of 1.9 cm diameter. The samples set into hard monoliths in approximately 2 h, but were allowed to cure for a full week before they were removed from the molds. They were then allowed to cure another 2 weeks and were then cut into lengths of 2 cm each.

Densities of the surrogate samples were determined by measuring the weight and volume, and open porosities were determined by the water intrusion method, in which samples were kept immersed in hot water at 70˚C for 4 h, cooled, and then wiped and weighed to determine the weight gain due to intrusion of the water in the open pores. Compression strength was measured on an Instron machine in a uniaxial compression mode; results are presented in Table 2.

To evaluate the leachability of the hazardous components the TCLP [24] test was carried out on these samples. The leaching levels were compared with the most stringent Universal Treatment Standard (UTS) of the U.S. Environmental Protection Agency (EPA) [27]. Results and passing limits are given in Table 3.

To test the retention of the hazardous and radioactive surrogate metals in the waste form over a long period of time in an aqueous environment, we conducted the American Nuclear Society's ANS 16.1 test [28]. The results of the test were expressed as the leaching index (LI), which is the negative logarithm of the diffusion constant, and are presented in Table 4.

To gain an insight into the microstructure and phase composition of the waste form, X-ray diffraction and scanning electron microscopy (SEM) were used. Because the actual waste may contain a reduced phase of Pu, we also prepared some Ce_2O_3 samples (in addition to the CeO_2 samples) to see the fate of the lower oxidation phases. The X-ray diffraction patterns for both the samples and the SEM photomicrograph for the CeO_2 surrogate waste form are given in Figs. 2 and 3, respectively.

To test the feasibility of incorporating Pu in these CBPC waste forms, three different waste

streams were selected; details are given in Table 5. The U-Pu oxide mixture was a result of corrosion of a U-Pu alloy. The TRU combustion residue was obtained originally from Rocky Flats. It was fully calcined for safe transport to our laboratory; as a result, all organics and combustibles were completely incinerated and the Pu content was enhanced. To study the radiolysis effects of the organic components of the wastes in the waste form, it was therefore necessary to add a polymer to the waste and produce suitable samples. It is not possible to simulate the almost-infinite variety of possible organic compounds in these surrogate wastes. Therefore, just to test the extent of radiolytic gas production in these ceramics, we added the Bakelite mounting compound, i.e., a phenol-formaldehyde resin, in the waste and produced the third waste.

Monolithic cylindrical samples were made in a nitrogen-flowing glovebox by following the procedure developed with the surrogate waste streams. Table 6 contains details of the proportions of the waste, binder, and water used in this study and also gives the actual Pu concentration in the final waste forms. In all cases, samples set in ≈2 h after the slurry was mixed for 30 min and then left undisturbed. There was no heating during mixing. The slurry thickened slightly because of some loss of water due to evaporation in the dry nitrogen glovebox.

The samples were allowed to cure for one week in the molds and then removed; they appeared homogeneous and dense. They were further cured for two more weeks, cut into geometrically regular cylindrical shapes, and then subjected to various tests.

Gas release studies were conducted on all stabilized Pu samples. The stabilized sample of the TRU combustible residue that had cured for only 7 days before undergoing gas generation studies to investigate the effect of curing on gas release. In addition, the same study was also conducted on the TRU combustible residue that was not stabilized. For each sample, a preweighed amount of sample (6.0-19.1 g) was loaded into a 100-mL Pyrex beaker that was then placed in one of a series of 300-cm^3 stainless steel high-pressure vessels manufactured by Parr Instrument Co. This minimized the potential for possible surface reactions with the stainless steel vessel wall. Each

vessel was sealed and leak-tested by evacuating the vessel and monitoring the pressure over a ≈2-3 h period. The vessel was assumed to be leak-tight if no change in pressure was observed. It was pressurized to approximately 1000 torr with nitrogen, evacuated, and repressurized to the same pressure. The dead volume, i.e., the gas phase, of each vessel was determined on the basis of the premeasured volume of the vessel less the volume of the beaker and the sample. The dead volume was 280-295 cm^3. The vessels were maintained in a once-through nitrogen atmosphere glovebox whose temperature was controlled at 25 ± 3˚C.

The vessels were sampled periodically by expanding the dead volume of the vessel into an evacuated manifold. The pressure of the vessel after expansion was recorded with a National Institute of Standards Technology traceable pressure gauge. The vessel was isolated from the manifold, and the content of the manifold was expanded into an evacuated gas-sampling vessel. The content of the gas sampling vessel was analyzed by gas chromatography using VARIAN Model 3300 and 3400 series gas chromatographs for H_2, O_2, N_2, CO, CO_2, CH_4 and N_2O. A limited number of samples were also analyzed for C_1, C_2, and C_3 hydrocarbons.

The water contents of the three CBPC samples listed in Table 6 are relatively similar (20.08-20.99 wt.%) and represent a significant percentage of the total weight of the waste form. To establish this water content as the main source of H_2, a sample of a Pu-laden CBPC (5.0 wt.% Pu and 18.9 wt.% H_2O) was dewatered by heating at 110 ± 5°C for 1 h in a dry nitrogen atmosphere. Based on the difference in weight of the sample before and after heating, the residual water content of the sample was calculated to be ≈1 wt.%. This is consistent with the results of differential thermal (DTA) and thermogravimetric analyses (TGA), which indicate that most of the water is removed from the CBPC samples at this temperature (see Fig. 1). Samples of the undewatered and dewatered Pu-laden CBPC were loaded into separate Parr vessels and the H_2 yield was measured. The results of this study are presented in Table 7 and in Figs. 6 and 7.

3. Results

MKP is a very durable phase of a very low aqueous solubility and a solubility product constant (pKsp) of 16 [29]. Its microstructure is highly crystalline, with crystallite sizes of 50-100 μm [30]. It is also a thermally stable product, as may be seen in the DTA and TGA plots given in Fig. 1. Except for the endotherm at 120˚C, the patterns show very stable phases at high temperature. At 120˚C, the loss in weight is ≈34 wt.%, the same as the stoichiometric proportion of water given by Eq. 1. This suggests removal of bound water at 120˚C. This quantitative result indicates that all bound water has escaped, leaving the matrix anhydrous. Heating larger monoliths beyond 120˚C also showed a similar loss in weight. Thus, the only transformation that occurs by lower-temperature heating is the loss of the water of hydration in which the material becomes anhydrous $MgKPO_4$. If needed, this comparatively low-temperature removal of water provides an inexpensive option of using an anhydrous matrix for Pu encapsulation. In this feasibility study, however, we did not resort to thermal treatment.

Typically, the density of cement grout is ≈2.4 g/cm^3. Compared to this, the density of 1.84 g/cm^3 of these waste forms (Table 2) is low and indicates that these materials are lightweight ceramics. The open porosity is also very low. Our earlier investigations [8] showed that the low density is partly a result of closed pores in these ceramics. These isolated pores do not contribute to the leaching of the contaminants nor do they allow intrusion of groundwater; hence, they are of no consequence to the leaching resistance of these ceramics. This closed porosity, estimated at ≈15 vol.%, could reduce the compression strength of the ceramics. Despite this, the compression strength is nearly twice that of cement grouts. According to the Land Disposal Requirements [25], compression strength should be >3.45 MPa, which the CBPC waste forms exceed by at least one order of magnitude.

The closed porosity may also contribute to gas generation from the final waste form if the isolated pores trap free water that is decomposed by the alpha radiation emitted by the Pu atoms.

For this reason, minimizing the isolated porosity is desirable. No attempt was made in this study to produce a denser product.

A comparison of the leaching levels and the universal treatment standard (UTS) [27] limits in Table 3 show that all of the metals pass this test. The actual levels are at least one order of magnitude lower than the UTS requirements. Despite the fact that the hazardous-metal levels in this surrogate waste are several thousand ppm, the leaching levels are extremely low. Because leaching levels are generally much lower (in the hundreds of ppm) in real waste streams, the actual waste forms should meet the UTS limits and the performance of the waste forms should not be sensitive to any minor variations in hazardous metals concentration in the waste streams or in waste loading in the final waste forms.

Nd and Ce are not hazardous metals and hence have no TCLP passing limits. Because they represent radioactive Pu and Am, respectively, we expect that performance of the waste form would be judged by their As Low As Reasonably Achievable (ALARA) leaching levels. In this respect, the observed levels below the detection levels of the instrument indicate that these waste forms may be most suitable for radioactive wastes. In particular, Ce concentration is several percent of the waste; this implies the feasibility of a nonleachable CBPC waste form that incorporates significant levels of TRU waste.

Table 4 lists the LI for the contaminants for Pb, Ba, and Ce. We could not calculate the LI for Cr, Ni, Cu, and Nd, because all measurements were below the detection limits of the instrument (as shown in the third column of Table 4) for these metals. For Pb, Ba, and Ce, the LIs are very high, ranging from 13.7 to 19.7. However, a good comparison of these values cannot be made with vitreous waste forms due to the lack of LI data in the literature for the same contaminants on glass. However, Bamba et al. [31] measured the diffusion constant for Cs and Sr in nuclear waste glass, obtaining values of 4.6×10^{-13} and 9.3×10^{-13} cm^2/s, which translate into LI for Cs and Sr as 12.34 and 12.03, respectively. The LIs found in this work are higher than these numbers. Taking

LIs of vitrious waste forms as a measure of good waste forms, one may conclude that the waste forms produced in this work show equal or better retention performance for Pb, Ba, and Ce. For Cr, Ni, Cu,and Nd, the fact that leaching levels are undetectable indicates that these ceramics exhibit superior retention of those contaminants. This conclusion is particularly important in the case of Ce because it represents radioactive Pu and because its nondetectable level in the ANS 16.1 test indicates that radioactive contaminants such as Pu are unlikely to leach out even in a long term leaching test.

Figure 2 shows the X-ray diffraction outputs of the waste forms made from surrogate wastes containing Ce as CeO_2 in (a) and Ce_2O_3 in (b), both with Ce at high concentrations of 5 wt.% in the waste. Both patterns display very sharp peaks of CeO_2 and no prominent peaks of Ce_2O_3. It appears that the pyrophoric Ce introduced in its lower oxidation state as Ce_2O_3 has fully oxidized into its most stable nonpyrophoric form of CeO_2 in the acidic environment of the phosphate slurry during the setting phase. Thus, it is likely that reduced phases of Pu from the waste will behave in a similar manner and will be converted to PuO_2 in the final waste forms.

The prominent peaks of CeO_2 also indicate that this phase has probably not been chemically converted into its more insoluble forms as phosphates. The low observed leaching of Ce is due to the very low solubility of CeO_2 itself (pK_{sp} = 47.7).

In addition to the chemical immobilization, superior microencapsulation is evident from the dense matrix seen in the photomicrograph of the matrix shown in Fig. 3. The dense matrix microencapsulates the individual metal components, hence superior retention of the contaminants is seen in the leaching tests. Thus, in addition to the chemical immobilization of the contaminants, this dense structure offers superior physical encapsulation.

One sample that contained combustion residue without organics (to represent actual waste) was used to estimate density and open porosity and was subjected to X-ray diffraction studies. The density was 1.954 g/cm^3 and open porosity was 10.78 vol.%. The X-ray diffraction pattern is

given in Fig. 4. The tests for the density and porosity were the same as those conducted on surrogate samples and given in Table 2, but done on only one sample this time and hence was only a rough estimate. Both the density and open porosity are slightly higher than those observed in the surrogate waste forms. The higher density is due to the higher atomic weight of Pu relative to that of Ce and also because the Pu content in the waste form was higher than that of Ce. The higher open porosity may occur because of the difference between surrogate and actual waste composition. The surrogate waste is formed by adding oxides of metals. These oxides readily participate in the chemical reaction and hence in the bonding. In real wastes, however, some of these oxides are part of the silicates that are less reactive and may simply be physically encapsulated without any chemical reaction. This difference between surrogate and real waste is likely to lead to a difference in the connected porosity.

In Fig. 4, sharp peaks of PuO_2 and residual MgO are noticeable. The residual MgO is typical of these phosphate ceramic matrices (see also Fig. 2). During the setting reaction, the MgO grain surfaces react with the acid phosphate, leaving the inner core of the grains unreacted. On the other hand, due to the very poor solubility of PuO_2, most of this compound remains unreacted and therefore we see its clear occurrence in the X-ray diffraction pattern. Thus, while MgO reacts on the grain surfaces to form part of the matrix, the PuO_2 particles are microencapsulated without chemically reacting with the phosphates.

This microencapsulation is evident in the SEM photomicrographs presented in Fig. 5, which contains direct and back-scattered images at two different magnifications. The bright grains in the back-scattered images are Pu. They are not clearly visible in the direct image because they are covered by a thin layer of phosphate glassy matrix; this cover is best noticed when one compares the direct image and back-scattered images (5c and 5d) at the higher magnification. One may notice in the lower-magnification photomicrographs (5a and 5b) that Pu is well scattered in the matrix. The sizes of the Pu grains vary, and grains measuring only a few micrometers to 20 μm are noticeable. Their physical encapsulation by the phosphate matrix may be seen in the higher-

magnification images. The grain is well embedded in the matrix and no separation between them is noticeable, implying that the phosphate matrix encapsulates the Pu particles very tightly in the matrix.

The gas generation due to ionizing radiation in these samples occurs mainly due to Pu-239, which is an alpha emitter. All samples with Pu generated H_2 while no O_2 was detected from any samples. A small amount of CO_2 was generated by the sample of TRU combustible residue without the Bakelite compound, and small amounts of CH_4 and CO were generated by the CBPC sample containing a mixture of the TRU combustible residue and the Bakelite compound. The G values, defined as the radiation chemical yield to the energy absorbed expressed in terms of the number of molecules generated per 100 eV of energy absorbed, are given in Table 7. The numbers of molecules of H_2 generated as a function of the total decay energy, defined as the product of the number of decays in a given time period and the average energy of the emitted alpha particle per decay for each radionuclide present in that sample, are shown in Fig. 6. The decay energy was calculated on the basis of the isotopic compositions of the samples. Because the $G(H_2)$ value for alpha radiolysis of liquid water is ≈4 times that for gamma radiolysis [32], only alpha radiolysis was considered and we assumed that 100% of the decay energy is deposited in the sample. We have assumed that 100% of the decay energy is deposited into the entire mass of the sample.

In general, a linear relationship has been observed between the number of molecules of H_2 generated and the total decay energy emitted by all three CBPC samples. The H_2 yield for the CBPC sample containing the U-Pu oxide mixture is 0.13 molecule of H_2/100 eV, while the same for the TRU combustible residue is 0.10 molecule of H_2/100 eV (Table 7). The relationship between H_2 yield and the total decay energy emitted is slightly more complicated for the CBPC sample containing the mixture of TRU combustible residue and Bakelite compound. Initially, a nonlinear relationship was observed with the H_2 yield that decreased as the total emitted decay energy increased to $\approx 0.83 \times 10^{22}$ eV (equivalent to 8 days). As the total emitted decay energy increases above this value, a linear relationship is observed between the number of molecules of H_2

generated and the total decay energy emitted with a H_2 yield of 0.23 molecule of H_2/100 eV. The H_2 yield has been constant for a period of time (i.e., in terms of total decay energy emitted) equivalent to at least 10 times the initial period during which the H_2 yield decreased as the total decay energy emitted increased. During this initial period, the average H_2 yield was 0.57 molecule of H_2/100 eV (Table 7). For comparison, the TRU combustible residue not incorporated in CBPC has an H_2 yield of 0.007 molecule of H_2/100 eV.

As shown in Fig. 7, the H_2 yield observed for the dewatered sample is significantly lower than that (by one order of magnitude) observed for the undewatered sample. Because no changes in the physical or structural properties of CBPC were observed after heating to 110°C, it would be feasible to process CBPC at this temperature before placing the waste form in the canister in order to significantly reduce the rate of H_2 generation.

4. Discussion

The various performance tests discussed above demonstrate that CBPC waste forms are viable alternatives to existing technologies for stabilization of TRU-waste combustion residues. The main advantages of the CBPC process are its simplicity, low cost, room-temperature nature, and as been shown in our earlier work [30], the fact that combustion residues themselves react in the setting reaction to provide a hard and dense ceramic.

Our earlier studies on hazardous contaminants such as Pb and Hg [33] have indicated that these metals are immobilized chemically in these ceramics and are simultaneously microencapsulated physically. Contrary to this, PuO_2 is only physically microencapsulated in these ceramics. This difference in behavior of hazardous contaminants such as Pb and radioactive contaminants such as Pu (i.e., one is available for chemical immobilization and other is not) is due to the difference in dissolution characteristics of these contaminants. An insight in this difference may be gained from the following specific example of solubility considerations of Pb and Pu stabilization.

Figure 8 contains the theoretical solubilities (pC) of Pu, Pb, and Mg in the pH range of the acid-base reaction of the CBPC process. The solubility values for Pb and Mg have been calculated from their literature values of the solubility product constants (Ksp) as10^{-14} and $1.3x10^{-13}$, respectively [34]. The solubility curve for Pu, on the other hand is reproduced from Puigdomenech and Bruno [35] who calculated the values from the Ksp value of 10^{-56}. In practice, the theoretical and experimentally measured solubilities often differ slightly in certain pH ranges, as measured values depend on the presence of other solutes in the solutions. For example, Puigdomenech and Bruno [35] indicate that the actual solubility of Pu is significantly higher in the pH range between 3 and 5, but otherwise is very close to the theoretical values. Similarly, the solubility of Mg in certain mineral wastes such as bauxite tailings measured by Thornber and Hughes [36] is not as high in the acidic range of pH as the theoretically predicted value. Despite such differences, it is still useful to use the theoretical values to reach general conclusions on the fate of the contaminants in the CBPC matrix.

When MgO is mixed with KH_2PO_4 solution to form the CBPC matrix, the pH of the solution increases steadily from the initial value of 4 as the alkaline MgO dissolves in it. At the onset of formation of the CBPC matrix, the pH reaches 8.5. Thus, during the 30 min of mixing of the slurry, the hazardous and radioactive contaminants are subjected to the pH range of 4 to 8.5. In this pH range, solubility of Pb is considerably higher than that of Pu and hence Pb reacts and is stabilized as a less-soluble $PbHPO_4$; however, Pu is not available for chemical conversion in a soluble form because of its very low solubility and remains unaltered and eventually is microencapsulated in the CBPC matrix. Thus, the excellent performance of the hazardous metals in the TCLP and ANS 16.1 tests is a result of the chemical conversion of these metals into their insoluble phosphate forms, but the extreme leaching resistance of Pu in the ANS 16.1 test is a result of its very low solubility. This example demonstrates that more soluble hazardous contaminants are readily available for chemical immobilization in the setting reaction than those that are less soluble, but less soluble TRU components are less leachable because of their poor solubility and both types of the contaminants are immobilized simultaneously in the same matrix.

The H_2 yields observed in the various CBPC samples compare well with $G(H_2)$ reported in the literature for alpha and gamma radiolysis in similar waste forms. They are comparable to $G(H_2)$ of 0.6 molecule of H_2/100 eV for a concrete investigated for solidification of tritiated water [10], 0.095 ± 0.005 total molecule/100 eV for the total gas production in FUETAP concrete [11], and 0-0.43 total molecule/100 eV (combined alpha and gamma radiolysis) for simulated Hanford current acid waste (CAW) and double-shell slurry (DSS) wastes immobilized in a cement-based grout [12]. Siskind [37] summarized the $G(H_2)$ values reported in the literature for cement-solidified low-level wastes (LLW) exposed to gamma radiation, which range from 0.03 to 0.35 molecule of H_2/100 eV. Draganic and Draganic [32] reported $G(H_2)$ values for the radiolysis of pure liquid water as a function of the linear energy transfer (LET). For Pu-239, $G(H_2)$ is 1.6 molecular H_2/100 eV. The values given in Table 7 for waste streams without organics compare well with these reported G values.

Radiolysis of pore water in the CBPC is the primary source of H_2, although radiolysis of organic material, if present, may also contribute to H_2 yield. For water, the primary reaction pathways for H_2 generation in the radiolytic decomposition of water [37] are as shown below.

$$2e_{aq}^- + 2H_2O \text{ ----> } 2\,H + 2OH^- \quad (2)$$

$$e_{aq}^- + H + H_2O \text{ ----> } H_2 + OH^- \quad (3)$$

$$H + H \text{ ----> } H_2\,. \quad (4)$$

O_2 is not a primary radiolytic product, but is generated by secondary reactions of oxygen-containing intermediates and products, such as the reaction of perhydroxyl radicals (Eqs. 5-6) (see Ref. 37). Significantly less O_2 should be generated relative to H_2 because oxygen-containing transients will react with other waste form constituents before they can build high-enough concentrations in solution to form O_2.

$$OH + H_2O_2 \text{ ----> } H_2O + HO_2 \quad (5)$$

$$2HO_2 \text{ ----> } H_2O_2 + O_2 . \quad (6)$$

$$OH + H_2 \text{ ----> } H_2O + H. \quad (7)$$

As noted above, O_2 has not been observed in any of the samplings to date.

H_2 is consumed by the reaction with OH radicals (Eq. 7). In a closed system, the rate of H_2 formation (Eqs. 2-4) will eventually equal the rate of H_2 decomposition (Eq. 7), which leads to the establishment of a constant, steady-state pressure [37].

Bibler and Orebaugh [10] reported that steady-state H_2 pressure increases with increasing dose rate. Both the rate of H_2 formation (Eqs. 2-4) and rate of H_2 decomposition (Eq. 7) increase with increasing dose rate; however, the rate of H_2 formation (Eqs. 2-4) increases faster because it involves two radicals. The steady-state pressure also increases with increasing LET until at very high LET, such as the recoil nucleus from the $^{10}B(n,\alpha)^7Li$ reaction, water is continuously decomposed and a steady-state pressure is not observed [38]. Although the G-value is a function of LET [32,38], it is independent of dose rate [10]. In an open system, a steady-state concentration of H_2O_2 is observed, with H_2 and O_2 generated continually as H_2O_2 decomposes; the net effect is decomposition of water into a stoichiometric ratio of its components [38].

Bibler and Orebaugh [10] reported steady-state H_2 pressures ranging from <140 kPa for dose rates of $<10^3$ Gy/h to ≈345 kPa for dose rates of 10^5 Gy/h for gamma-irradiated concretes. A steady-state pressure of ~207 kPa was observed for FUETAP concrete at a dose rate of 5.6×10^3 Gy/h irradiated for 55,000 dose-equivalent years with ^{244}Cm [4]. Our experimental objective for these experiments was to measure the H_2 yield as a function of decay energy for the Pu-laden CBPC samples. Our procedure is not suited for measuring steady-state pressure. Based on the work of Bibler and Orebaugh [10] and McDaniel and Delzer [4], a steady-state pressure of less than 140 kPa would be anticipated for Pu-laden CBPC samples for an estimated dose rate of ≈5 x

10^2 Gy/h (assuming 100% of the alpha decay is deposited in the sample).

McDaniel and Delzer suggested that radiolytic gaseous production is dependent on the amount of free or unbounded water within the pore volume of the FUETAP cement-based waste forms and that removal of this water should reduce the gaseous product yield [4]. For FUETAP cement with a 15 wt.% water content, a G value of 0.095 ± 0.005 total molecule/100 eV is observed. The G value decreases to 0.001-0.008 total molecule/100 eV if the cement is autoclaved at 250˚C for 24-h, which reduces the water content to ≈2 wt.%. Based on these results, McDaniel and Delzer estimated that a negligible pressure increase would be observed in a 200-L drum filled to 90% capacity with a dewatered FUETAP waste form during the first 1000 years at a dose rate of 5.6 x 10^3 Gy/h. This suggests that pressure buildup due to radiolytic gases in the CBPC waste forms with a similar behavior may not be a significant issue during transportation and storage.

As noted in the discussion, a small amount of CO_2 was generated by the sample with TRU combustible residue. This sample contained ash (see Table 6) which had a residual carbon content of 0.08 wt.%. It is likely that this C was oxidized by the OH radicals that yielded this small amount of CO_2. Such CO_2 is not likely to accumulate in the dead volume of the canister, as it will react with residual MgO to produce $MgCO_3$. Small quantities of CH_4 and CO have been detected in the dead volume of the CBPC sample containing the mixture of TRU combustible residue and Bakelite powder. The CH_4 yield is 8 x 10^{-3} molecular CH_4/100 eV. The CO yield is 4 x 10^{-3} molecular CO/100 eV. These yields have been much smaller than those resulting from the decomposition of water and hence will not contribute to the overall yield of gases in the canister.

5. Conclusions

This feasibility study has demonstrated that the CBPC waste forms chemically immobilize hazardous contaminants and physically microencapsulate both hazardous contaminants and Pu in a hard ceramic matrix. The investigations on Ce and Pu indicate that the radioactive contaminants are stabilized as four valent oxide forms that are not leachable. The waste forms meet the current

Safeguard Termination Limit as determined by DOE [26] on Pu that requires that the Pu be stabilized as PuO_2, one of the least soluble phases of Pu. Investigations reported here on surrogate Ce indicates that oxidation of Pu from Pu_2O_3 to PuO_2 removes its pyrophoricity, thus making the waste form safer for transportation and storage. The gas generation studies conducted in this work with actual wastes indicates that the gas yield is minimal and does not result in pressurizing the waste containers. Thus, the CBPC waste forms conform to WIPP waste acceptance criteria. These positive attributes make this technology a viable room-temperature alternative for stabilization of Pu-contaminated ashes.

Acknowledgments

This project was funded by the U.S. DOE Mixed Waste Focus Area and Plutonium Focus Area under Contract W-31-109-Eng-38. The authors thank Y. Macheret of DOE for recognizing the role of the CBPC process in the stabilization needs of the TRU wastes and for drawing our attention to its potential. Discussions with D. Maloney and G. Thompson of the Kaiser Hill Company at Rocky Flats Technology Center have helped in interpretation of some of the data given in this paper. The authors thank Sylvia Hagamann for help in preparing the final manuscript, and C. Malefyt for efficient technical editing.

References

[1] R.G. Behrens, E.C. Buck, N. L. Dietz, J.K. Bates, E. Van Deventer, and D.J. Chaiko, Characterization of Plutonium-Bearing Wastes by Chemical Analysis and Analytical Electron Microscopy, Argonne National Laboratory Report ANL-95/35 (1995).

[2] I.W. Donald, B.L. Metcalfe, and R.N.J. Taylor, Review of the Immobilization of High Level Radioactive Wastes Using Ceramics and Glasses, Journal of Materials Science 32 (1997) 5851-5887.

[3] W.C. Rask and A.G. Phillips, Ceramification: A Plutonium Immobilization Process, in Proc. U.S. DOE Pu Stabilization and Immobilization Workshop, Dec. 12-14 (1995) 153-157.

[4] E.W. McDaniel and D.B. Delzer, Fuetap Concrete, Chapter 9 in Radioactive Waste Forms for the Future, eds. W. Lutze and R.C. Ewing, Elsevier Science Pub. (1988) pp. 565-588.

[5] S.Y. Jeong, A.S. Wagh, and D. Singh, Chemically Bonded Phosphate Ceramics for Stabilizing Low-Level Radioactive Wastes, To appear in Proc. 98th Annual Meeting of American Ceramic Soc., Indianapolis, April 14-17, 1996.

[6] A.S. Wagh, S.Y. Jeong, D. Singh, R. Strain, H. No, and J. Wescott, Stabilization of Contaminated Soil and Waste Water with Chemically Bonded Phosphate Ceramics, in Proc. Waste Management Annual Meeting, 97, Tucson (1997), available at http:www.wmsym.org/wm97proceedings/

[7] D. Singh, V. Mandalika, A. Wagh, R. Strain, and M. Tlustochowicz, Immobilization of ^{99}Tc in Low-Temperature Phosphate Ceramic Waste Forms, Ceramic Trans., Vol. 87, Environmental Issues and Waste Management Technologies, in Ceramic and Nuclear Industries III, eds. D. K. Peeler and J. C. Marva (1998) 653-664.

[8] D. Singh, D. Barber, A.Wagh, R. Strain, and M. Tlustochowicz, Stabilization and Disposal of Argonne-West Low-Level Mixed Wastes in Ceramicrete™ Waste Forms, to appear in Proc. Waste Management '98 Conf., Tucson, March 1-5, 1998.

[9] V. Maio, R. K. Biyani, R. Spence, G. Loomis, G. Smith, and A. Wagh, Testing of Low-Temperature Stabilization Alternatives for Salt Containing Mixed Wastes - Approach and Results to Date, to appear in Proc. Spectrum '98, Amer. Nucl. Soc., LaGrange, IL (1998).

[10] N. E. Bibler and E. G. Orebaugh, “Radiolytic Gas Production from Tritiated Waste Forms - Gamma and Alpha Radiolysis Studies,” Report No. DP-1459, Savannah River Laboratory (1977).

[11] G. Dole, G. Rogers, M. Morgan, D. Stinton, J. Kessler, S. Robinson and J. Moore, “Cement-Based Radioactive Waste Hosts Formed Under Elevated Temperatures and Pressures (FUETAP Concrete) for Savannah River Plant High-Level Waste,” Report No. ORNL/TM-8579, Oak Ridge National Laboratory (1983).

[12] L. R. Dole and H. A. Friedman, “Radiolytic Gas Generation from Cement-Based Waste Hosts for DOE Low-Level Radioactive Wastes,” Report No. CONF-860605-14, Oak Ridge National Laboratory (1986).

[13] B. Siskind, “Gas Generation from Low-Level Waste,” Report No. WM-3175-16, Brookhaven National Laboratory (1991).

[14] A. R. Kazanjian, “Radiolytic Gas Generation In Plutonium Contaminated Waste Materials,” Report No. RFP-2469, Rocky Flats Plant, Golden, CO (1976).

[15] M. A. Molecke, “Gas Generation from Transuranic Waste Degradation: Data Summary and Interpretation. Report No. SAND-79-1245, Sandia National Laboratories (1979).

[16] D. T. Reed, J. Hoh, J. Emery, and D. Hobbs, "Radiolytic Gas Production in the Alpha Particle Degradation of Plastics," in Proc. of Waste Management 92, Vol. 2, pp. 1081-1085 (1992).

[17] D. T. Reed and M. A. Molecke, “Generation Of Volatile Organic Compounds By Alpha Particle Degradation Of WIPP Plastic And Rubber Material,” in Proc. of Symp. on Scientific Basis for Nuclear Waste Management XVII, Vol. 333, pp. 233-240, 1993.

[18] D. T. Reed, J. Hoh, J. Emery, S. Okajima, and T. R. Krause, “Gas Production Due To Alpha Particle Degradation of Polyethylene And Polyvinylchloride,” Report No. ANL-97/7, Argonne National Laboratory (1997).

[19] J. P. Ryan, “Radiogenic-Gas Accumulation in TRU Waste-Storage Drums,” Report No. DP-1604, Savannah River Laboratory (1982).

[20] F. G. Smith, III, “A Computer Model of Gas Generation and Transport Within TRU Waste Drums,” Report No. DP-1754, Savannah River Laboratory (1988).

[21] R. Lappin, R. L. Hunter, D. P. Garber, and P. B. Davies, “Systems Analysis, Long-term Radionuclide Transport, and Dose Assessments, Waste Isolation Pilot Plant (WIPP), Southeastern New Mexico; March 1989,” Report No. SAND89-0462, Sandia National Laboratories (1989).

[22] L. H. Brush, “Position Paper: Gas Generation in the Waste Isolation Plant,” Report No. CONF-941244-1, Sandia National Laboratories (1994).

[23] U.S. EPA, Resource Conservation and Recovery Act. PL94-580. (1976). Superfund Treatability Study Protocol: Identification/Stabilization of Soils Containing Metals. Phase II Review Draft, Office of Research and Development, Cincinnati, and Office of Emergency and Remedial Response, Washington, DC (1990).

[24] U.S. EPA, Method 1311, Toxicity Characteristics Leaching Procedure (TCLP) (1992) Rev. II, pp. 138-139.

[25] Mayberry, T. L. Harry, and L. M. DeWitt. Technical-Area Status Report for Low-Level Mixed Waste Final Forms, Vol. I, DOE/MWIP-3,1992.

[26] Pu Recoverability Testing, Version 3.0, U.S. DOE, Oct. 1, 1997.

[27] EPA 40 CFR Part 268 in Sept. 1994 for Treated Wastes.

[28] American Nuclear Soc., American National Standard Measurement of the Leachability in Solidified Low-Level Radioactive Wastes by a Short-Term Test Procedure. Method ANSI/ANS 16.1-1986, American Nuclear Soc., La Grange Park, IL 1986.

[29] A.W. Taylor, A.W. Frazier, and E.I. Gurney, Solubility Products of Magnesium Ammonium and Magnesium Potassium Phosphate, Trans. Faraday Soc., Vol. 59 (1963) 1580.

[30] A.S. Wagh, S.Y. Jeong, and D. Singh, High-Strength Phosphate Ceramic (Cement) Using Industrial By-Product Ash and Slag, Proc. of International Conf. on High-Strength Concrete, Kona, HI (July 1997).

[31] T. Bamba, H. Kamizono, S. Nakayama, H. Nakamura, S. Tashiro, "Studies of Glass Waste Form Performance at the Japan Atomic Energy Institute," in Performance of High Level Waste Forms and Engineered Barriers Under Repository Conditions, International Atomic Energy Agency Report IAEA-TECDOL-582 (1991) 165-190.

[32] G. Draganic and Z. D. Draganic, The Radiation Chemistry of Water, Academic Press, New York (1971).

[33] A.S. Wagh, S.Y. Jeong, and D. Singh, Mercury Stabilization in Chemically Bonded Phosphate Ceramics, To appear in Proc. Amer. Ceram. Soc. Fall Meeting, San Antonio, Oct. 30-Nov. 2, 1996, Pub. Amer. Ceram. Soc., Westerville, OH.

[34] W.F. Linke, Solubilities of Inorganic and Metal Organic Compound, American Chemical Society (1965).

[35] I. Puigdomenech and J. Bruno, Plutonium Solubilities, Tech. Report 91-04. Swedish Nuclear Fuel and Waste Management Co., Stockholm (1991).

[36] M.R. Thornber and C.A. Hughes, The Mineralogical and Chemical Properties of Red Mud Waste from the Western Australian Alumina Industry, in Bauxite Tailings, eds. A.S. Wagh and P. Desai, Pub. Univ. West Indies, Kingston, Jamaica (1987) 1-19.

[37] B. Siskind, "Gas Generation from Low-Level Waste: Concerns for Disposal," Report No. BNL-NUREG-47144, Brookhaven National Laboratory (1992).

[38] J. W. T. Spinks and R. J. Woods, *An Introduction to Radiation Chemistry*, 3rd Ed., John Wiley & Sons, Inc., New York (1990) pp. 255-269.

Table 1
Surrogate waste composition (wt.%)

Component	Al_2O_3	Nd_2O_3	B_2O_3	BaO	CaO	Cr_2O_3	CuO	Fe_2O_3	K_2CO_3	MgO	MnO_2
Oxide	3.33	0.098	1.66	1.077	4.01	0.78	1.077	5.48	1.145	4.41	0.098
Hazardous or surrogate metal	-	0.08	-	0.964	-	0.536	0.862	-	-	-	-
Component	NaOH	NiO	K_3PO_4	PbO	SnO	Ta_2O_5	TiO_2	C	SiO_2	CeO_2	-
Oxide	1.39	0.489	1.468	0.88	0.098	0.294	1.66	18.5	41.02	11.3	-
Hazardous or surrogate metal	-	0.385	-	0.857	-	-	-	-	-	9.2	-

Table 2
Physical properties of surrogate sample

Physical property	Measured value
Density (g/cm^3)	1.84
Open porosity (vol.%)	4.4
Compression strength (MPa)	60 ± 5

Table 3
Toxicity characteristic leaching levels for surrogate waste form (mg/L)

Element	Ba	Cr	Cu	Ni	Pb	Ce	Nd
Leaching level	0.68	0.01	0.04	<0.05	<0.10	<0.05	<0.05
UTS limit	1.2	0.86	-	5.00	0.37	-	-

Table 4
Leaching index and detection limits for hazardous contaminants and radioactive surrogates

Contaminant	Leaching index	Lower than leaching levels (μg/L)
Pb	13.7	---
Cr	---	10
Ni	---	30
Ba	14.9	---
Cu	---	10
Ce	19.7	---
Nd	---	0.04

Table 5
Test waste streams, their characteristics, and Pu content

Waste stream	Origin and characteristics	Content of Pu and other actinides
Mixture of U and Pu	U-Pu alloy, an Argonne inventory item, fully oxidized and formed into fine powder.	75 wt.% U and 25 wt.% Pu
TRU combustion residue	Originally from Rocky Flats; subsequent operations led to high Pu concentration. Fine powder residue.	31.8 wt.% Pu as PuO_2 with minor content of reduced phase of Pu. ^{241}Am = 0.1 wt.%. ^{39}Pu = 90%, ^{240}Pu = 8.4%, ^{241}Pu = 1.3%.
TRU combustion residue with addition of phenol-formaldehyde resin	63.7 wt.% mounting compound was added to combustion residue to study gas generation in waste form that will contain 10 wt.% organics.	19.4 wt.% Pu as PuO_2 in combustion residue, with minor content of reduced phase of Pu. ^{241}Am = 0.06 wt.%. ^{239}Pu = 90 %, ^{240}Pu = 8.4%, ^{241}Pu = 1.3%.

Table 6
Components used in fabrication of waste forms, and final Pu content (wt.%)

	Components in starter mixture				
Sample identity	Waste	Binder	Water	Class-C fly ash	Pu content
U-Pu oxide mixture	20.98	58.94	20.08	None	5.245
Combustion residue	24.75	31.65	20.99	22.61	7.87
Combustion residue with Bakelite compound	15.7 waste and 10 Bakelite compound	31.65	20.99	21.63	5.00

Table 7
Samples investigated in gas generation studies. All G values calculated assuming 100% of decay energy is deposited into entire mass of sample. Details of these samples are given in Tables 2 and 3.

Sample	wt.% Pu	G Value (molecular H_2/100 eV	(molecular H_2 • g Sample) (100 eV.gH_2O)
CBPC containing U-Pu oxide mixture	5.245	0.13	0.65
CBPC containing TRU combustible residue	7.87	0.10	0.48
CBPC containing TRU combustible residue	5.00	0.23[1]	1.1[1]
CBPC containing TRU combustible residue and Bakelite compound	31.8	31.8	NA

[1]G(H_2) observed for >0.83 x 10^{22} eV of total decay energy released. An average of 0.57 molecular H_2/100 eV was observed for 0 to 0.83 x 10^{22} eV of total decay energy released.

LIST OF FIGURES

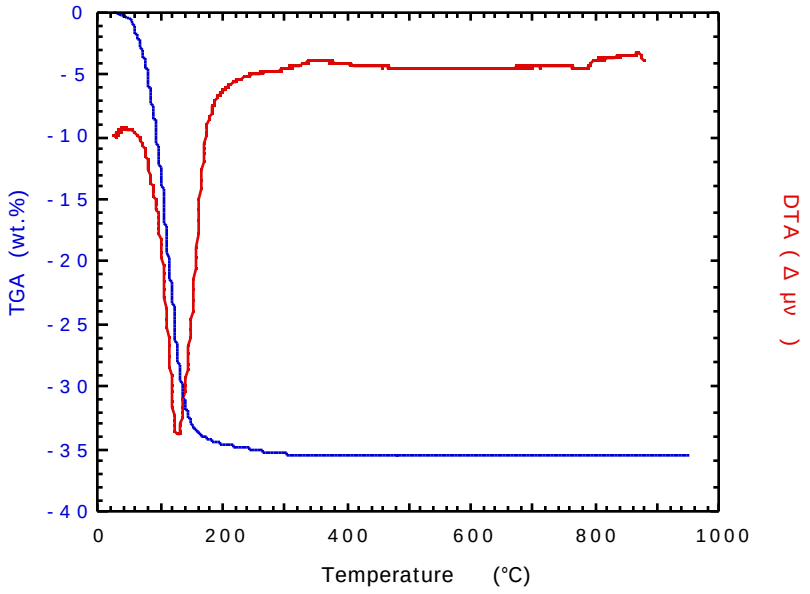

Fig. 1. Differential thermal and thermogravimetric plots of matrix material.

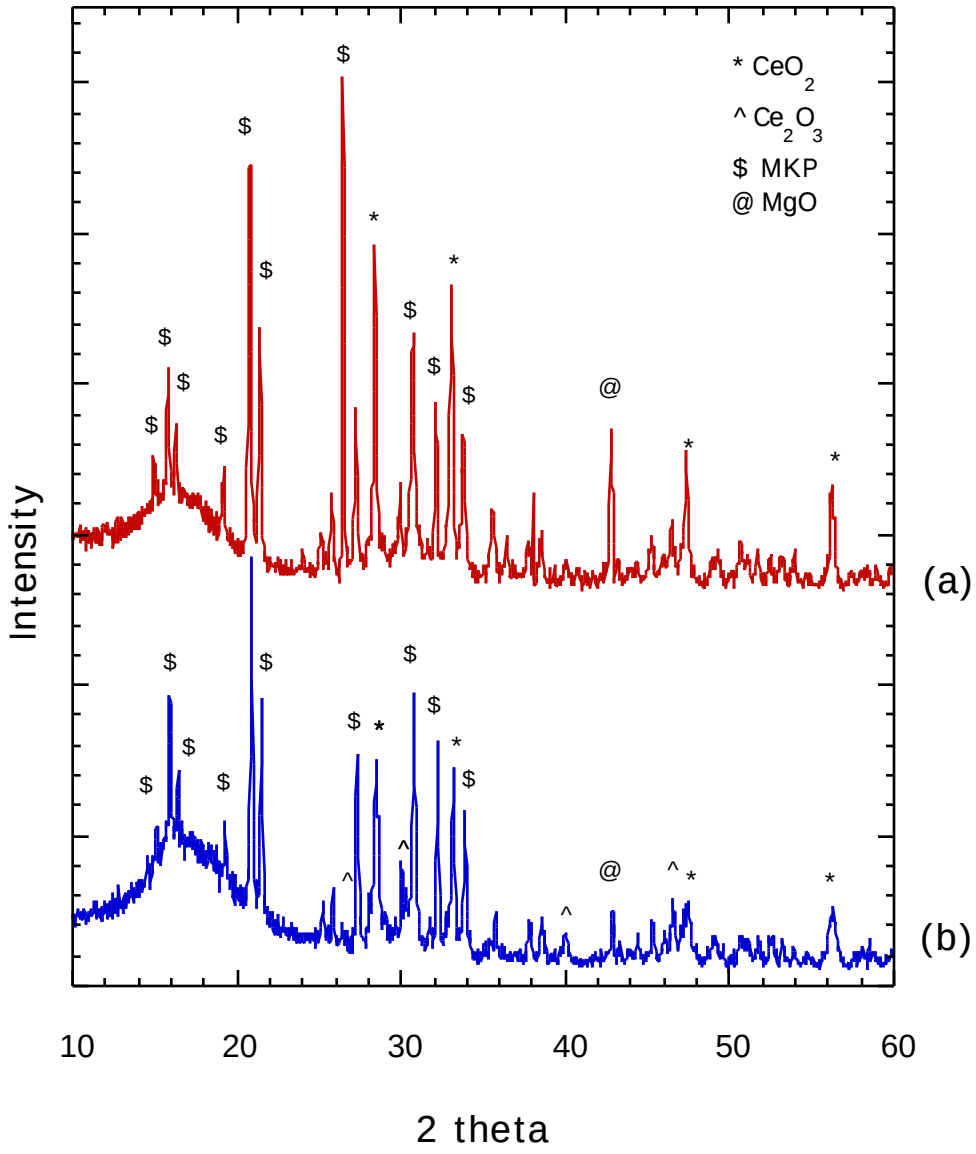

Fig. 2. X-ray diffraction patterns of waste forms containing (a) CeO_2, and (b) Ce_2O_3 as surrogates of PuO_2 and Pu_2O_3.

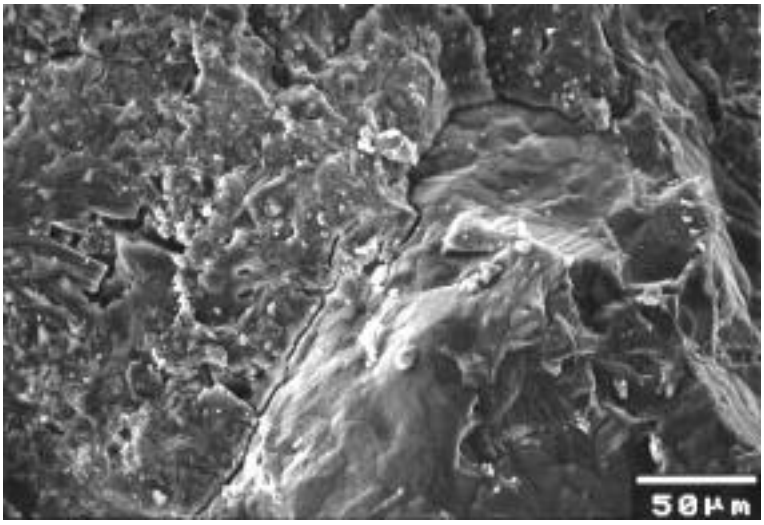

Fig. 3. SEM photomicrograph of surrogate waste form.

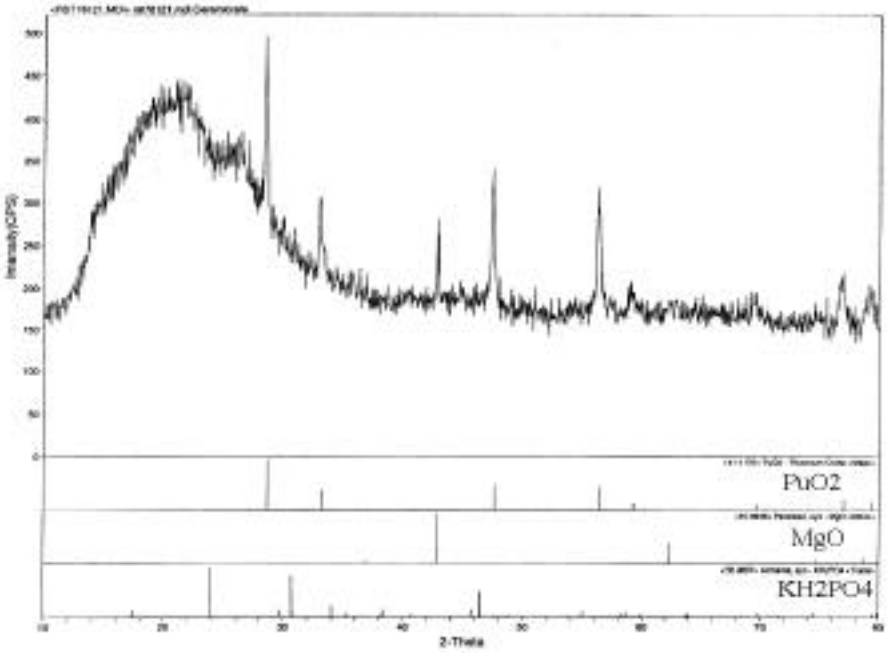

Fig. 4. X-ray diffraction pattern of waste form of combustion residue without organics.

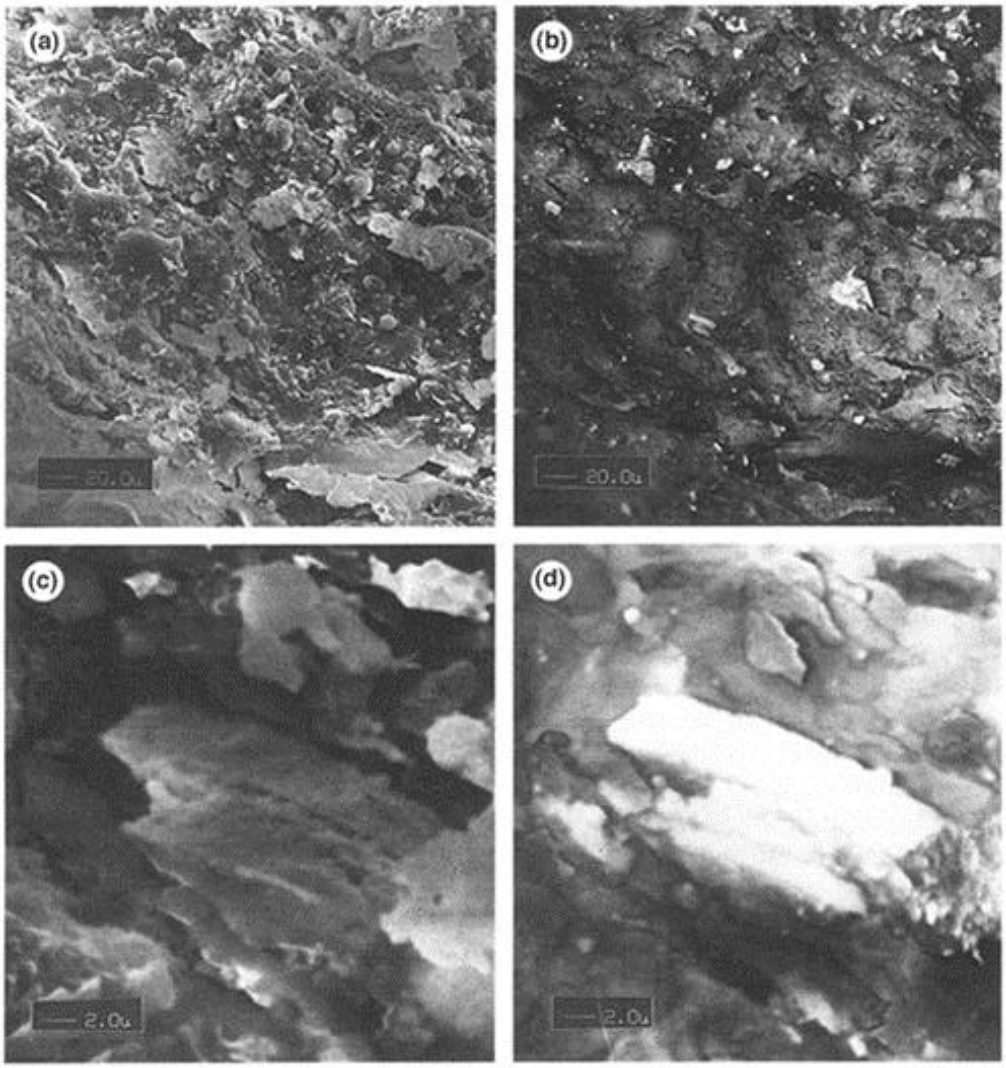

Fig. 5.

SEM photomicrographs of fractured surface of waste form of combustion residue without organics: (a) direct image at low magnification, (b) back-scattered image at low magnification, (c) direct image at high magnification, and (d) back-scattered image at high magnification.

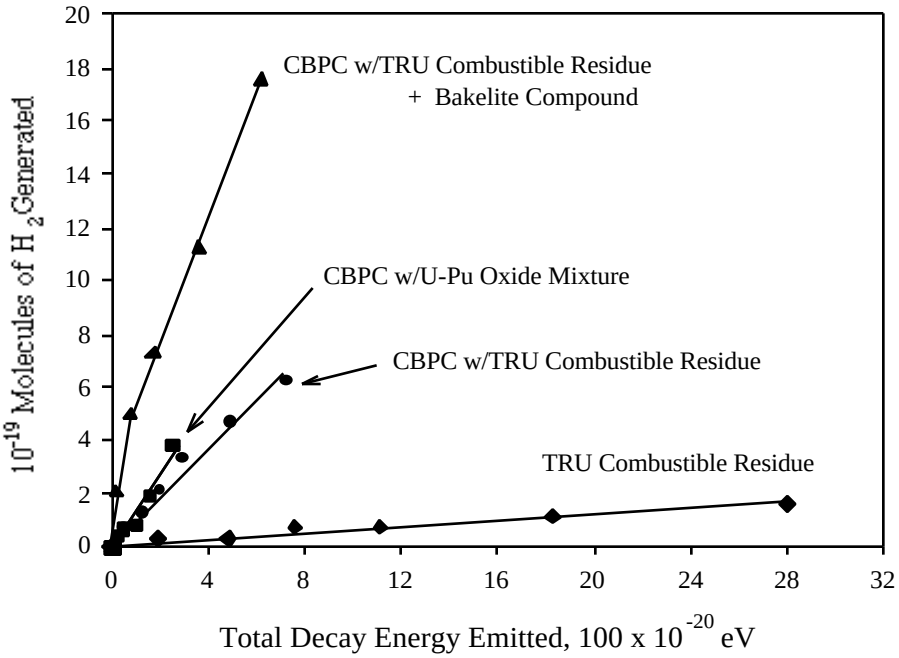

Fig. 6. Molecules of H_2 generated by radiolysis for the three Pu-laden CBPC samples and a sample of TRU combustible residue.

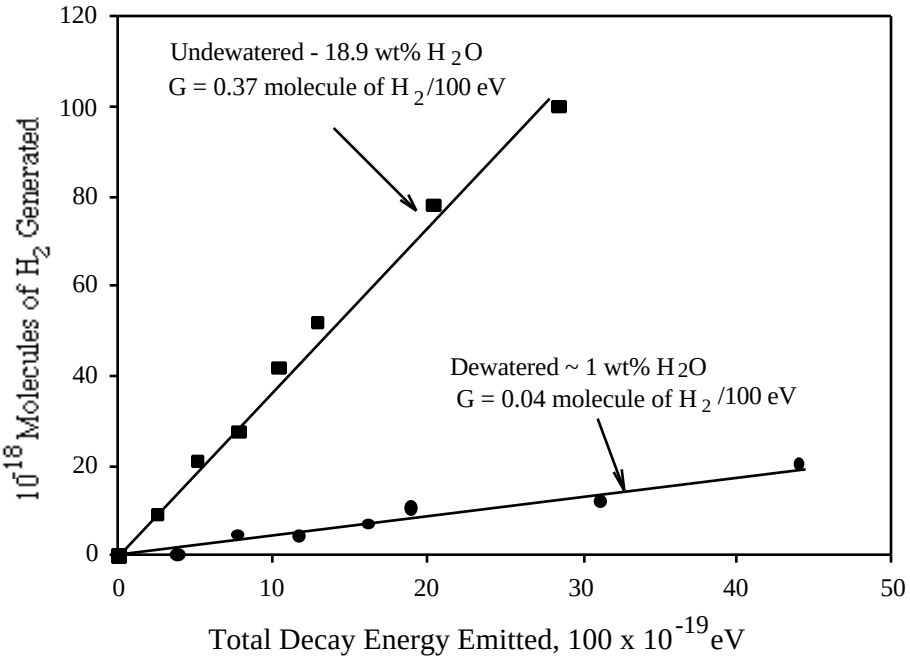

Fig. 7. Effect of water content on the rate of radiolytic H_2 generation for a Pu-laden CBPC sample. Dewatering was accomplished by heating a sample of the Pu-laden CBPC at 110 ± 5°C.for 1-h in a nitrogen atmosphere.

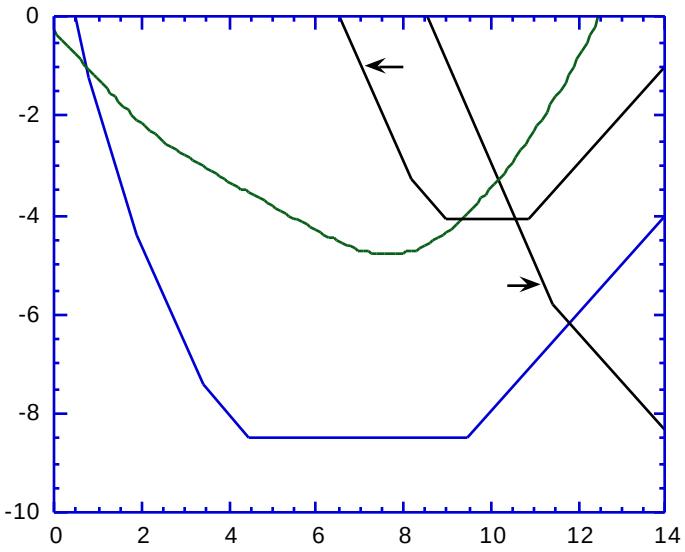

Fig. 8. Dissolution characteristics of Pu, Pb, and Mg in acid-base reaction of CBPC process.